*Journal of Statistical Physics, Vol. 62, Nos. 3/4, 1991*

# Recurrence of Kolmogorov–Arnold–Moser Tori in Nonanalytic Twist Maps

**Bambi Hu,[1] Jicong Shi,[1] and Sang-Yoon Kim[2]**

*Received July 13, 1990*

We study a class of twist maps where the function $g(\theta) = \theta(1 - |2\theta|^{z-1})$ is nonanalytic ($C^1$) and endowed with a varying degree of inflection $z$. When $z > 3$, reappearance of a KAM torus after its breakup has been observed. We introduce an "inverse residue criterion" to determine the reappearance point. Scaling behavior at the transition points is also studied. For $2 \leqslant z < 3$ the scaling exponents are found to vary with $z$, whereas for $z \geqslant 3$ they are independent of $z$. In this sense $z = 3$ plays a role quite similar to that of the upper critical dimension in phase transitions.

**KEY WORDS:** Invariant circles; KAM tori; twist map; recurrence; scaling; universality; critical exponent; phase transition; nonanalyticity.

## 1. INTRODUCTION

The basic methodology in the study of the breakup of KAM tori was introduced by Greene in his 1979 paper.[1] However, even to this date, it is not clear how general the conclusions are beyond the standard map. Nevertheless, the methodology seems to have worked amazingly well in a wide range of problems.

In the context of the standard map the picture for the breakup of KAM tori is relatively simple. Each rotational torus is characterized by an irrational winding number. These tori serve as barriers to locally stochastic motion. However, as the perturbation strength is increased, more and more of these tori break up. At a critical perturbation value, the last KAM torus characterized by the "golden-mean" winding number breaks up, and global

[1] Department of Physics, University of Houston, Houston, Texas 77204-5504.
[2] Department of Physics, Kangwon National University, Kangwon-Do 200-701, Korea.



0022-4715/91/0200-0631$06.50/0 

stochasticity will set in. The famous residue criterion was introduced by Greene to determine very precisely the transition point.

In many aspect the breakup of KAM tori is analogous to a phase transition. By utilizing concepts and techniques used in the study of phase transitions, remarkable progress has been made in the understanding of the breakup of KAM tori. In particular, universal scaling exponents[2,3] characterizing the transition have been discovered.

In phase transitions diverse physical system can be divided into equivalence classes according to certain criteria. These universality criteria are well known in phase transitions. However, in contradistinction to phase transitions, much less is known about universality in chaotic transitions. Nevertheless, we know, for example, in the case of period doubling, the critical-point order[4] is one of the universality criteria on which the scaling exponents depend.

To gain a better understanding of universality, we have recently studied the circle map, which can be viewed as the dissipative limit of the standard map. The circle map is generally used to model the quasiperiodic transition to chaos. In this case the degree of inflection $z$ serves a universality criterion. The sine function in the circle map possesses a cubic inflection point ($z=3$). To generalize it to any arbitrary degree of inflection, a polynomial function which is nonanalytic ($C^1$) was invented.[5,6] The scaling exponents are found to depend monotonically on $z$, and their asymptotic limits as $z \to \infty$ have also been found.[6]

To examine the problem of universality in the conservative case, we similarly replace the sine function in the standard map by this polynomial function. To our amusement we found that $z=3$ plays a role quite similar to that of the upper critical dimension in phase transitions, i.e., the scaling exponents are dependent on $z$ for $2 \leqslant z < 3$, and yet independent of $z$ for $z \geqslant 3$.

The most interesting part of this investigation was, however, the phenomenon of the recurrence of KAM tori.[7-9] The "golden-mean" KAM torus is found to reappear after it has broken up. However, this is true only for $z > 3$; no such reappearance has been observed for $z \leqslant 3$. Although we have only observed a finite number of reappearances, it can conceivably recur infinitely many times. We have proposed an "inverse residue criterion" for the determination of the reappearance point, which is complementary to the "residue criterion" for the determination of the disappearance point.

This paper is organized as follows. In Section 2 we write down the class of nonanalytic twist maps and discuss their symmetry properties. In Section 3 we study the breakup of KAM tori. In Section 4 the problem of scaling and universality is investigated. In Section 5 a summary is given.

## 2. NONANALYTIC TWIST MAPS

In this paper, we study a class of twist maps

$$T: \begin{cases} r_{i+1} = r_i - kg(\theta_i) \\ \theta_{i+1} = \theta_i + r_{i+1} \end{cases} \tag{1}$$

where $\theta_i \in [-1/2, 1/2)$ and $r_i \in [0, 1]$. We choose[5,6] $g(\theta) = \theta(1 - |2\theta|^{z-1})$, where $z$ denotes the degree of inflection at $\theta = 0$. $g(\theta)$ is periodically extended by defining $\theta$ modulo 1. Hence,

$$g(\theta + \tfrac{1}{2}) = g(\theta - \tfrac{1}{2}) \tag{2}$$

$$g(\tfrac{1}{2}) = g(-\tfrac{1}{2}) = 0 \tag{3}$$

Since $g(\theta)$ is a $C^1$-function, $T$ represents a class of nonanalytic twist maps. Figure 1 plots $g(\theta)$ for some values of $z$ and the function $(1/2\pi)\sin(2\pi\theta)$. Since the extrema of $g(\theta)$ are no longer symmetrically located at $\theta = 1/4$ or $\theta = -1/4$ for $z \neq 2$, $T$ is not invariant under a change of sign of $k$ and a shift of $\theta$. Therefore, we have to study both parameter regions $k > 0$ and $k < 0$.

The periodic orbits have rational winding numbers $\omega_i = P_i/Q_i$, i.e., $\theta_{Q_i} = \theta_0 + P_i$ and $r_{Q_i} = r_0$. The stability properties of the periodic orbits can be characterized by the residue,

$$R_i = \tfrac{1}{4}[2 - \mathrm{Tr}(DT^{Q_i})] \tag{4}$$

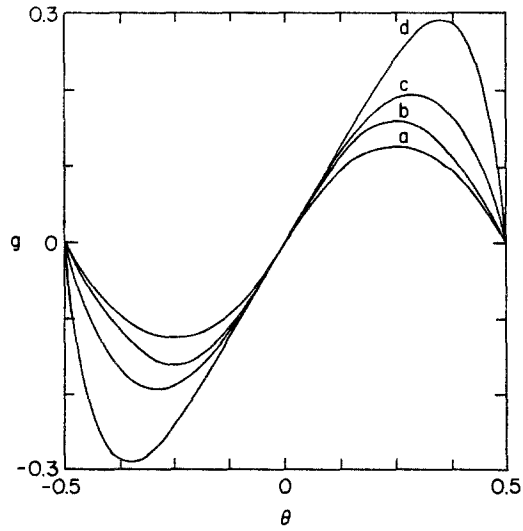


Fig. 1. The function $g(\theta)$. (a) $z = 2$; (b) $(1/2\pi)\sin(2\pi\theta)$; (c) $z = 3$; (d) $z = 6$.

where $DT^{Q_i}$ is the linearized matrix of $T^{Q_i}$. An elliptic orbit has $0 < R_i < 1$, and a hyperbolic orbit has $R_i < 0$ or $R_i > 1$. Since $g(\theta)$ is an odd function, the map is reversible, i.e., it can be written as a product of two involutions

$$T = I_2 I_1 \tag{5}$$

where

$$I_1: \begin{cases} r' = r - kg(\theta) \\ \theta' = -\theta \end{cases} \tag{6}$$

$$I_2: \begin{cases} r' = r \\ \theta' = r - \theta \end{cases} \tag{7}$$

Since each involution possesses two symmetry lines, there are altogether four symmetry lines:

$$\text{a.} \quad \theta = -1/2 \tag{8}$$

$$\text{b.} \quad \theta = 0 \tag{9}$$

$$\text{c.} \quad \theta = (r-1)/2 \tag{10}$$

$$\text{d.} \quad \theta = r/2 \tag{11}$$

For a particular rational winding number, each orbit (elliptic or hyperbolic) has two points on two of these four lines. One line will be mapped to another at the halfway point of the orbit. The pattern of how these lines map into each other is called a *routing pattern.*

A KAM torus with an irrational winding number $\omega$ can be approximated numerically by a sequence of periodic orbits whose winding numbers are the successive convergents of the continued fraction expansion of $\omega$. The particular KAM torus we will focus our attention on is the one whose winding number is the inverse of the "golden-mean," $\omega = (\sqrt{5}-1)/2$. Its convergents are $\omega_i = F_i/F_{i+1}$, where $F_i$ is the $i$th Fibonacci number, which satisfies $F_{i+1} = F_i + F_{i-1}$ with $F_0 = 0$, $F_1 = 1$. Using this approximation, we found that $T$ still has a dominant symmetry line within a certain interval of $k$.

In two-dimensional area-preserving maps which model two-degree-of-freedom Hamiltonian systems, KAM tori act as one-dimensional barriers that prevent the trajectories from diffusing from one region to another. When the parameter exceeds a certain critical value, the last KAM torus breaks up and becomes a cantorus. A cantorus acts as a partial barrier, and diffusion occurs. The theory of transport based on the action variational principle can be used not only to predict the diffusion rate, but also

to examine the existence of a KAM torus. For the map (1) the generating function is

$$F(\theta, \theta') = \frac{1}{2}(\theta - \theta')^2 + \frac{1}{2} k\theta^2 \left( \frac{2}{z+1} |2\theta|^{z-1} - 1 \right) \tag{12}$$

The action of the orbit with winding number $P_i/Q_i$ is

$$W_{P_i/Q_i} = \sum_{j=0}^{Q_i - 1} F(\theta_j, \theta_{j+1}) \tag{13}$$

For each winding number $P_i/Q_i$, there are at least two orbits: one minimax ($R_i > 0$) orbit and one minimizing ($R_i < 0$) orbit. The action difference between these two orbits

$$\Delta W_i = W^{\max}_{P_i/Q_i} - W^{\min}_{P_i/Q_i} \geqslant 0 \tag{14}$$

gives the area that is transported under one iteration of the map.

## 3. BREAKUP OF KAM TORI

In this work, we use the following two criteria to study the breakup of a KAM torus.

**1. Greene's Residue Criterion.** This criterion postulates a close relation between the existence of a KAM torus with an irrational winding number $\omega$ and the stability property of the period-$Q_i$ orbits as $P_i/Q_i$ approaches $\omega$. If a KAM torus exists for $k < k_D$ and disappears for $k > k_D$, then

$$\lim_{i \to \infty} R_i^{\pm}(k) = \begin{cases} 0^+, & k < k_D \\ R^{\pm}, & k = k_D \\ \pm\infty, & k > k_D \end{cases} \tag{15}$$

$R_i^{\pm}(k)$ are, respectively, the residues of the minimax (+) and minimizing (−) period-$Q_i$ orbits at a given value of the parameter $k$. The $R^{\pm}$ are two constants, and $|R^+| < 1$.

**2. Mather's Action-Difference Criterion.** Mather proved[10] that the necessary and sufficient condition for the existence of a KAM torus is $\Delta W_\omega = 0$. For the standard map, as $P_i/Q_i$ approaches $\omega$, $\Delta W_i$ decreases to zero for $k < k_D$, and tends to a nonzero constant for $k > k_D$.

In most cases Greene's criterion is a very effective numerical method to make a precise determination of $k_D$. Unfortunately, due to the lack of

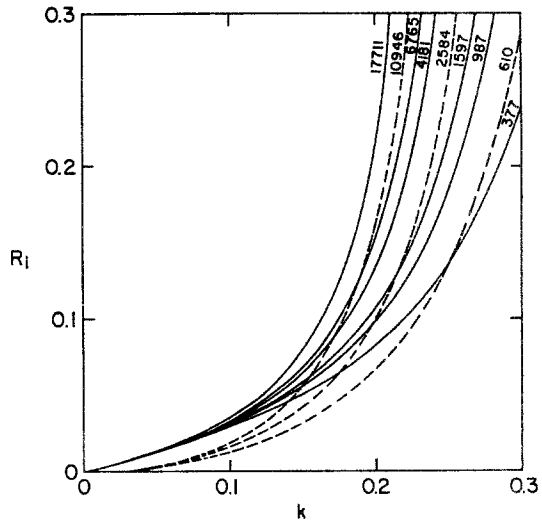


Fig. 2. The residue $R_l'$ as a function of $k$ for $z = 2$. The number on the curve indicates the period $Q_l$. The curves bunch into two groups for small $k$. The upper group has odd $Q_l$; the lower one, even $Q_l$. Both groups tend to zero as $k \to 0$.

a rigorous proof, the necessary and sufficient conditions for its validity is not known. Mather's criterion, on the other hand, was rigorously proved; and yet in practice it is very difficult to employ to make a precise determination of $k_D$. Nevertheless, Mather's criterion still serves as a very useful criterion to test the existence of a KAM torus. One can prove that no rotational invariant tori exist for $k \geqslant 2$ and $k \leqslant -2/(z-1)$. In the following,

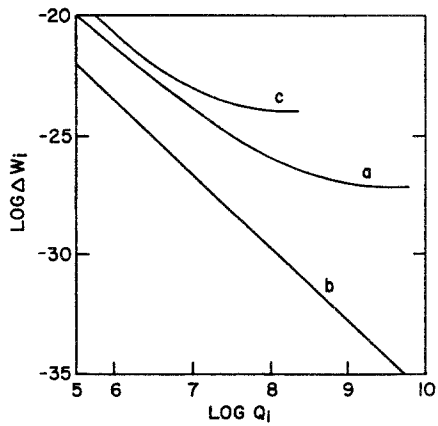


Fig. 3. Plot of $\log(\Delta W_l)$ vs. $\log(Q_l)$. (a) $z = 2$, $k = 0.3$; (b) $z = 2.1$, $k = 0.1$; (c) $z = 2.1$, $k = 1.174$. As $Q_l \to \infty$, the flux is nonzero for (a) and (c), but zero for (b).

we will discuss the behavior of the "golden-mean" KAM torus for different values of $z$. All computations were done in quadruple precision with 36 significant figures.

**(1) $k<0$ or $z\leqslant 2$.** Here we found that the dependence of the residues on the parameter $k$ is different from that of the standard map: for $k\neq 0$, $R_i^{\pm}\to\infty$ as $Q_i\to\infty$ (see Fig. 2 for a typical case). It is similar to the supercritical case ($k>k_D$) in the standard map. We have computed the action difference for several values of $k$. Figure 3 shows that the action difference tends to a nonzero constant as $Q_i\to\infty$. It suggests that there are no KAM tori when $k\neq 0$. As in the case of the sawtooth map, $k_D=0$ is the critical point for the breakup of the KAM torus. This is similar to a zero-temperature phase transition.

For $z\leqslant 2$ and $k>0$ the dominant symmetry line is $b$, and for $k<0$ the dominant symmetry line is $a$. These are the same as in the standard map. The residues are monotonic functions of $k$, and we did not observe any reappearance of KAM tori.

**(2) $2<z\leqslant 3$.** Using Greene's criterion, we found $k_D\neq 0$; however, no reappearance of KAM tori has been observed. From Fig. 4 we see that $k_D$ tends to zero monotonically as $z$ decreases from 3 to 2 (see Table III). This suggests that $k=0$ is the critical point for $z=2$. For $k$ in the vicinity of $k_D$, the dominant symmetry line is $b$.

**(3) $z>3$.** In this case the behavior of the "golden-mean" KAM torus is significantly different. We found that there is more than one value of $k$ which satisfies Greene's criterion. For example, for $z=4$, two disappearance points $k_D^{(1)}=1.4129353$ and $k_D^{(2)}=1.4261557$ have been found. If a

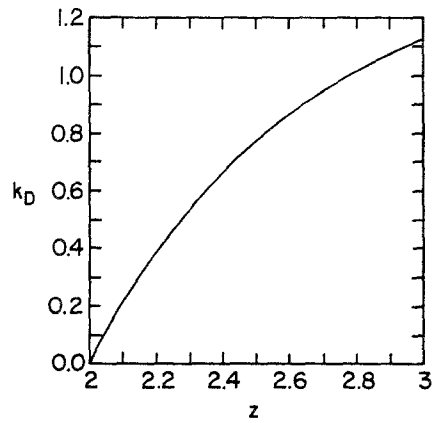


Fig. 4. The critical value $k_D$ as a function of $z$ for $2\leqslant z\leqslant 3$.

KAM torus disappears at two points, there must be a point $k_R$, $k_D^{(1)} < k_R < k_D^{(2)}$, at which it reappears. To find $k_R$, we propose an "inverse residue criterion" for the reappearance of a KAM torus:

*A KAM torus that has disappeared at $k_D$ will reappear at $k_R$ if*

$$\lim_{i\to\infty} R_i^{\pm}(k) = \begin{cases} \pm\infty, & k < k_R \\ R^{\pm}, & k = k_R \\ 0^{\pm}, & k > k_R \end{cases} \tag{16}$$

Using this "inverse residue criterion," we are able to make a precise determination of $k_R$. For $z = 3.8$, $k_R^{(1)} = 1.38760367$; for $z = 4$, $k_R^{(1)} = 1.42173415$. The superscript $(i)$ in $k_{D,R}^{(i)}$ refers to the $i$th time the KAM torus disappears ($D$) or reappears ($R$). We have also computed the action difference and found (see Fig. 5)

$$\begin{aligned} &\Delta W \to 0 && \text{if } k < k_D^{(i)} \text{ or } k_R^{(i)} < k < k_D^{(i+1)} \\ &\Delta W \to \text{const} > 0 && \text{if } k_D^{(i)} < k < k_R^{(i)} \text{ or } k > k_D^{(i+1)} \end{aligned} \tag{17}$$

These results together with the scaling behavior to be discussed in the next section suggest that $k_R$ is the point at which the "golden-mean" KAM torus reappears. Figure 6 shows the evolution of the phase portrait from

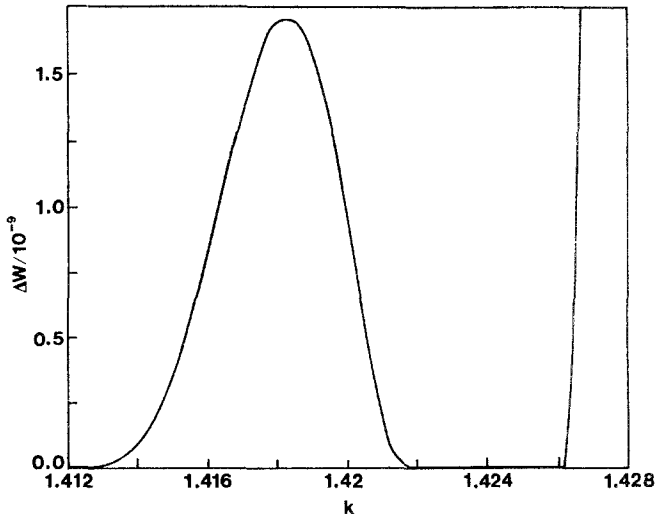


Fig. 5. The action difference $\Delta W$ as a function of $k$ for $z = 4$ and $(Q_i, P_i) = (1597, 987)$.

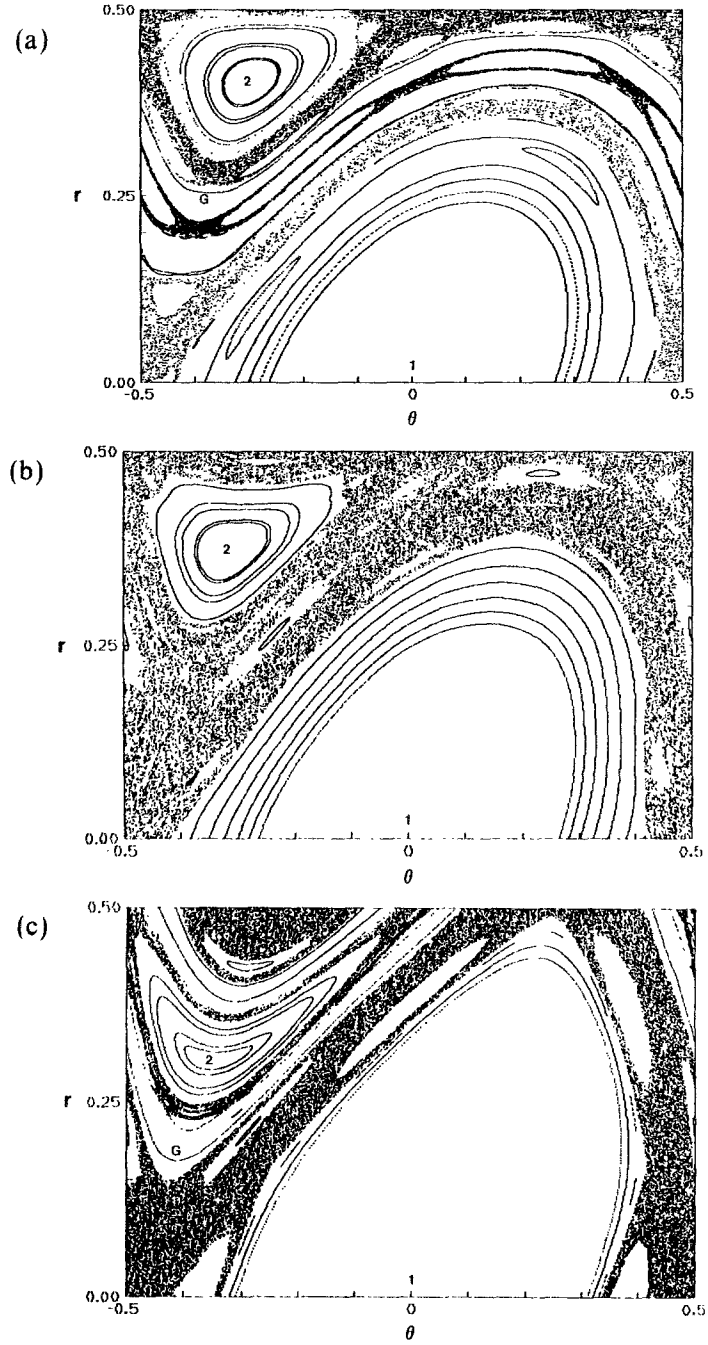


Fig. 6. Phase portraits from disappearance to reappearance of the KAM torus for the case $z = 6$. Here 1, 2, and G indicate, respectively, the period-1 resonance, period-2 resonance, and the "golden-mean" KAM torus. (a) $k = 0.704 < k_D^{(1)}$; (b) $k_D^{(1)} < k = 0.9 < k_R^{(1)}$; (c) $k_R^{(1)} < k = 1.35 < k_D^{(2)}$.

disappearance to reappearance of the KAM torus for the case $z = 6$. In Fig. 6a, $k < k_D^{(1)}$, the chaotic regions near the period-1 resonance and the period-2 resonance are separated by the KAM torus. In Fig. 6b, $k_D^{(1)} < k < k_R^{(1)}$, the KAM torus has disappeared and the chaotic regions become connected. In Fig. 6c, $k_R^{(1)} < k < k_D^{(2)}$, the KAM torus has reappeared and the chaotic regions become separated again.

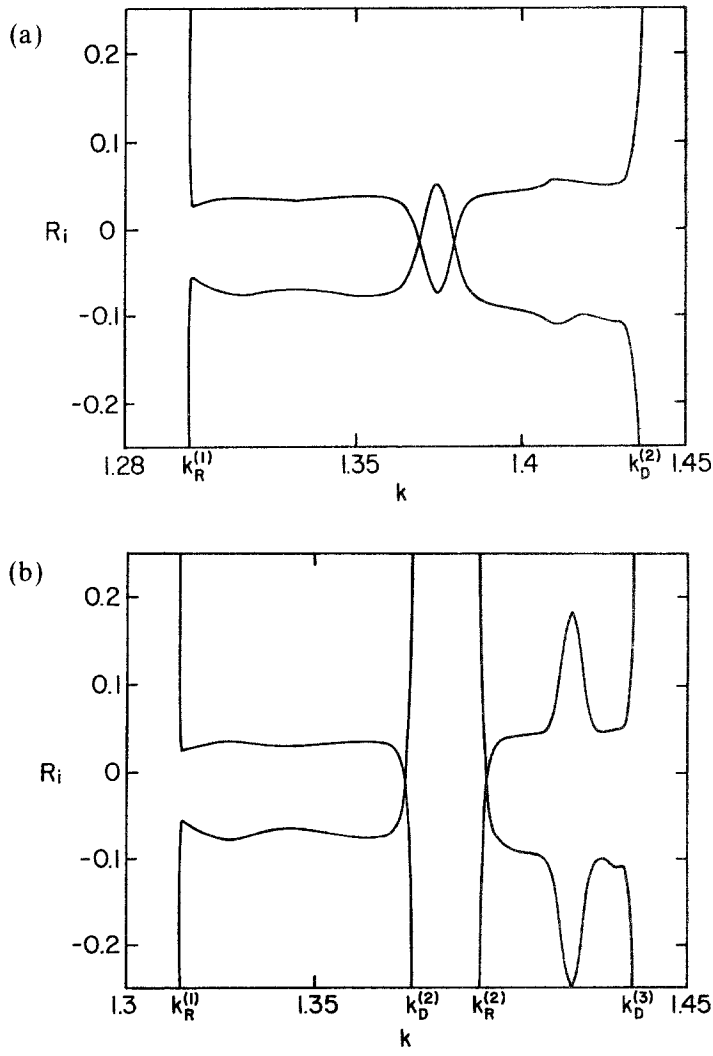


Fig. 7. The residue $R_i$ for $(Q_i, P_i) = (610, 377)$. (a) $z = 6$; (b) $z = 6.1$; (c) $z = 6.2$.

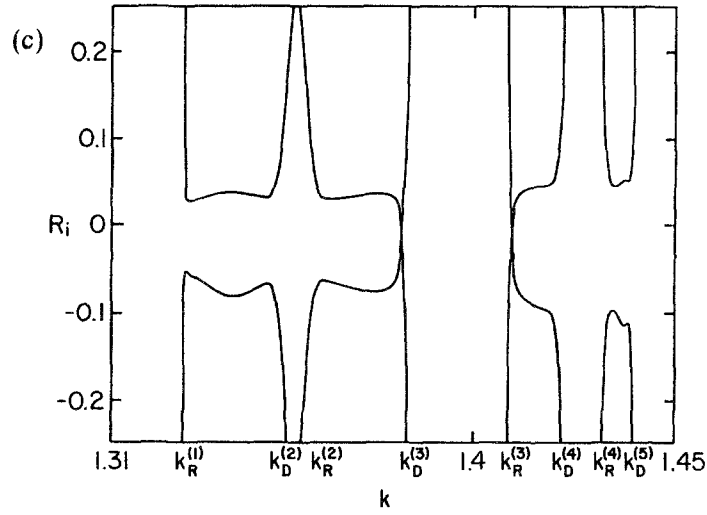


Fig. 7. (*Continued*)

It should be emphasized that a KAM torus can recur more than one time. For example, for $z=6$ we have observed that it recurs at least twice. The residues are no longer monotonic functions of $k$. They tend to infinity right after the KAM torus has broken up, and become finite again as the KAM torus reappears. Since we cannot ascertain the existence of a "final" breakup, the KAM torus can conceivably recur infinitely many times. When $z$ is a fraction, the dependence of the residues on $k$ is more complicated. From Fig. 7 we observe that as $z$ varies, there is a "bifurcation" of the regions in which KAM tori exist. This "bifurcation" is caused by the emergence of a pair of disappearance and reappearance points.

When the system makes the transition from $z=3$ to $z>3$, the situation is much more complicated. Take $z=3.1$ as an example. Figures 8 and 9 show how the residue of the orbits with different periods varies as a function of $k$. All these orbits have a common symmetry line $b$. Near $k=0$, $R_i<0$ for even-period orbits, and $R_i>0$ for odd-period orbits. It can be seen that the residue of any orbit decreases to the lowest negative value and then goes to positive infinity. As the period $Q_i$ is increased, the minimum of the residue moves to the right and its absolute value increases. From Table I we see that for a given $k$ the residue will change from positive to negative as the period is increased. The larger the value of $k$, the higher the period at which $R_i$ changes sign. We cannot find a point that satisfies Greene's criterion here. However, the results of the action difference (see Fig. 3) show that the "golden-mean" KAM torus exists as long as $k$ is small

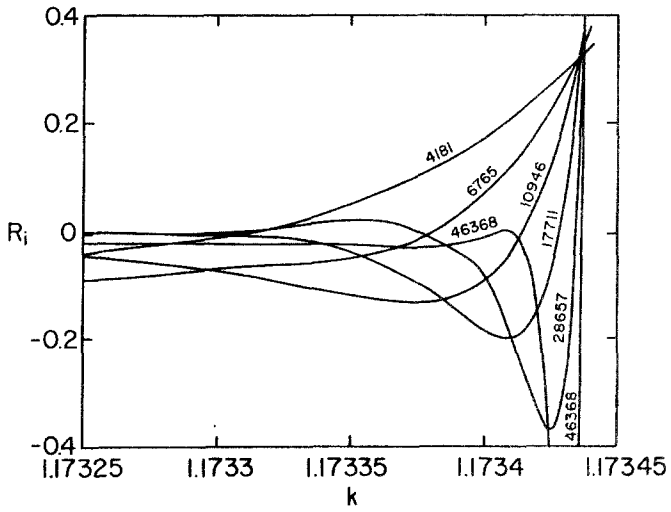


Fig. 8. The residues $R_i$ vs. $k$ for $z = 3.1$. The number on the curve indicates the period.

enough, but ceases to exist when $k$ is sufficiently large. It is not clear how to apply Greene's criterion here.

It should be noted that when there is a reappearance of the KAM torus the dominant symmetry lines may be different if $k$ is in the vicinity of $k_D^{(i)}$. A pair of disappearance and reappearance points have the same dominant symmetry line. For example, for $z = 4$, $d$ is the dominant sym-

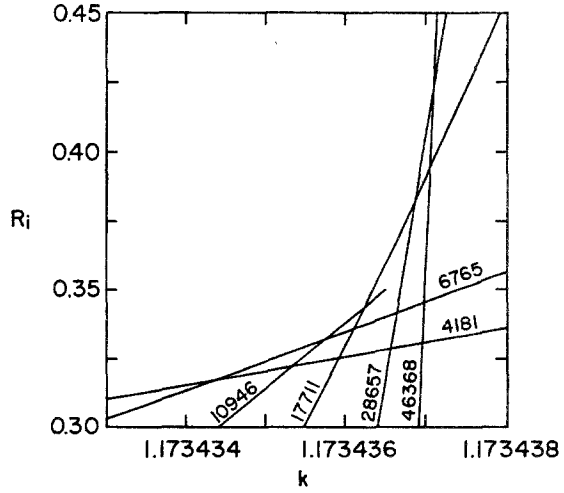


Fig. 9. A blowup of the upper right-hand corner of Fig. 8.

**Table I. Residue of Period-$Q_i$ Orbits for $z = 3.1$[a]**

| $Q_i$ | $k = 1.17342$ | $k = 1.173432$ | $k = 1.173436$ | $k = 1.1734365$ | $k = 1.173437$ |
|---|---|---|---|---|---|
| 4181 | 0.2503 | 0.3056 | 0.3258 | 0.3284 | 0.3310 |
| 6765 | 0.1894 | 0.2932 | 0.3346 | 0.3400 | 0.3456 |
| 10946 | 0.0573 | 0.2481 | 0.3380 | 0.3503 | 0.3630 |
| 17711 | −0.1440 | 0.1358 | 0.3300 | 0.3594 | 0.3902 |
| 28657 | −0.3358 | −0.1734 | 0.2401 | 0.3184 | 0.4041 |
| 46368 | −0.1641 | −0.8639 | −0.1766 | 0.0626 | 0.3566 |
| 75025 | 0.0890 | −0.4884 | −2.3977 | −1.5839 | −0.1858 |

[a] All orbits have a common symmetry line $b$. Given any $k$, the residue will change from positive to negative provided $Q_i$ is large enough.

metry line for $k \in (1{,}4, 1.414)$ and $(1.4217, 1.4218)$ (the vicinity of $k_D^{(1)}$ and $k_R^{(1)}$), whereas $c$ is the dominant symmetry line for $k \in (1.426, 1.4263)$ (the vicinity of $k_D^{(2)}$). From Table II one can see that there is an exchange of stability[8] between elliptic and hyperbolic orbits for an odd-period orbit as the parameter $k$ is increased from $k_R^{(1)}$ to $k_D^{(2)}$. Stability exchange usually occurs when there is a reappearance of KAM tori. However, in this case as well as the case $2 < z \leqslant 3$, we have observed an exchange of stability *before* the first breakup of the KAM torus. When $k$ is near zero, there is no dominant symmetry line, and the routing pattern is shown in Table II. At a certain value of $k$, an exchange of stability occurs, and a dominant symmetry line appears. Table II also shows what kind of orbit will change

**Table II. Routing Patterns for Orbits with Winding Number $P_i/Q_i$ when $k > 0$[a]**

| $Q_i$ | $P_i$ | $R_i$ | Before | After (I) | After (II) | After (III) |
|---|---|---|---|---|---|---|
| Odd | Even | $>0$ | $b \Leftrightarrow d$ | $b \Leftrightarrow d$ | $c \Leftrightarrow a$ | $d \Leftrightarrow b$ |
| | | $<0$ | $a \Leftrightarrow c$ | $a \Leftrightarrow c$ | $b \Leftrightarrow d$ | $a \Leftrightarrow c$ |
| Odd | Odd | $>0$ | $b \Leftrightarrow c$ | $b \Leftrightarrow c$ | $c \Leftrightarrow b$ | $d \Leftrightarrow a$ |
| | | $<0$ | $a \Leftrightarrow d$ | $a \Leftrightarrow d$ | $a \Leftrightarrow d$ | $b \Leftrightarrow c$ |
| Even | Odd | $>0$ | $c \Leftrightarrow d$ | $b \Leftrightarrow a$ | $c \Leftrightarrow d$ | $d \Leftrightarrow c$ |
| | | $<0$ | $a \Leftrightarrow b$ | $c \Leftrightarrow d$ | $a \Leftrightarrow b$ | $a \Leftrightarrow b$ |

[a] Before (after) refers to before (after) the first stability exchange. $\Leftrightarrow$ denotes how the symmetry lines are mapped to each other. There is no dominant symmetry line before stability exchange. The dominant symmetry lines for cases (I), (II), and (III) are, respectively, $b$, $c$, and $d$. The dominant symmetry line is $a$ if and only if $k < 0$.

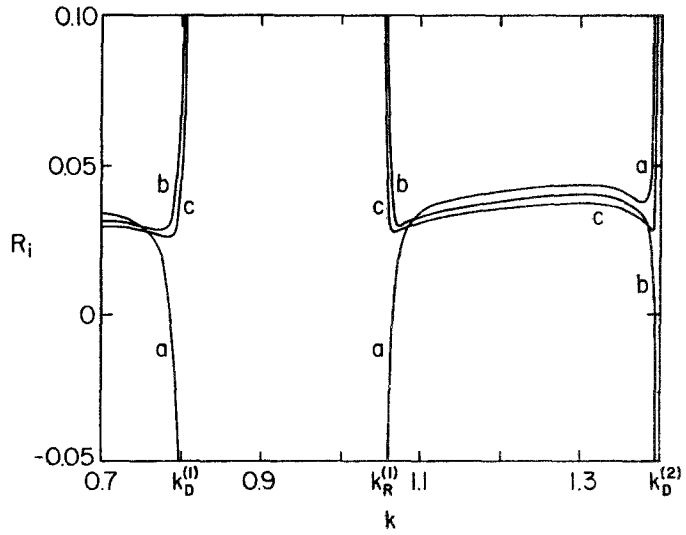


Fig. 10. The residues $R_i$ of the initially elliptic orbits for $z=5$. (a) $(Q_i, P_i)=(233, 144)$; (b) (377, 233); (c) (610, 377). The residues of the initially hyperbolic orbits are symmetrically located, and are not shown. Stability exchange occurs before the first breakup of the KAM torus for (a), but not for (b) and (c).

its stability as $k$ is increased from zero to the vicinity of $k_D^{(1)}$. Figure 10 shows the variation of the residues with $k$. It is evident here that stability exchange does not necessarily entail the reappearance of a KAM torus.

## 4. SCALING AND UNIVERSALITY

We first summarize the definitions of various scaling exponents. For a pair of minimax and minimizing orbits with winding number $P_i/Q_i$, we relabel and order the orbit elements as follows:

$$\theta_{Q_i}(1)<\theta_{Q_i}(2)<\cdots<\theta_{Q_i}(2Q_i-1)<\theta_{Q_i}(2Q_i) \tag{18}$$

where $\theta_{Q_i}(t)$ is minimax for $t$ odd, and minimizing for $t$ even. The distance between two neighboring points is

$$d_i(t)=\theta_{Q_i}(t)-\theta_{Q_i}(t+1) \tag{19}$$

Period-1 scaling is defined by

$$\begin{aligned}\frac{d_i(t)}{d_{i+1}(t)} &\sim \left(\frac{Q_i}{Q_{i+1}}\right)^{-x^{(1)}(t)} \\ \frac{r_i(t)-r_{i-1}(t)}{r_{i+1}(t)-r_i(t)} &\sim \left(\frac{Q_i}{Q_{i+1}}\right)^{y^{(1)}(t)}\end{aligned} \tag{20}$$

and period-3 scaling is defined by

$$\frac{d_i(t)}{d_{i+3}(t)} \sim \left(\frac{Q_i}{Q_{i+3}}\right)^{-x^{(3)}(t)}$$
$$\frac{r_i(t)-r_{i-3}(t)}{r_{i+3}(t)-r_i(t)} \sim \left(\frac{Q_i}{Q_{i+3}}\right)^{-y^{(3)}(t)} \tag{21}$$

where $x^{(i)}(t)$ and $y^{(i)}(t)$ with $i=1$ or 3 are the scaling exponents. For convenience, the exponents on the dominant symmetry line are denoted by $x_s^{(i)}$ and $y_s^{(i)}$; and the exponents on the symmetry line $l$ ($l=a, b, c, d$) are denoted by $x_l^{(i)}$ and $y_l^{(i)}$. For the standard map[2] it was found that $x_s^{(1)}=0.721$, $y_s^{(1)}=2.329$, $x_a^{(3)}=1.093$, $y_a^{(3)}=2.329$, and $x_s^{(1)}+y_s^{(1)}=x_a^{(3)}+y_a^{(3)}=3.05$ at the critical point of the breakup of the "golden-mean" KAM torus.

We have calculated the scaling exponents on the symmetry lines at the critical points of disappearance and reappearance of the "golden-mean" KAM torus for several values of $z$. For $k<0$ or $z\leqslant 2$ the critical point is $k_D=0$, and the system is integrable. The scaling exponents can be calculated analytically: $x^{(1)}(t)=1$ and $y^{(1)}(t)=2$. This is just the scaling behavior of a linear system. For $2<z<3$, we found that the scaling exponents at the critical point $k_D$ vary with $z$ (see Table III and Figs. 11 and 12). For $z=3$ the scaling behavior is the same as that of the standard map. Therefore, the scaling behavior changes smoothly from that of a linear system to that of the standard map as $z$ varies from 2 to 3. The sum of the exponents, $x^{(i)}+y^{(i)}$, which is a more useful quantity in the study of transport, shows a slightly increasing trend. However, the increase is too

**Table III. Disappearance Points $k_D$ and the Scaling Exponents for $2\leqslant z\leqslant 3$**

| $z$ | $k_D$ | $x_s^{(3)}$ | $y_s^{(3)}$ | $x_s^{(3)}+y_s^{(3)}$ | $x_c^{(3)}$ | $y_c^{(3)}$ | $x_c^{(3)}+y_c^{(3)}$ |
|---|---|---|---|---|---|---|---|
| 2.0 | 0 | 1 | 2 | 3 | 1 | 2 | 3 |
| 2.1 | 0.219 | 0.965 | 2.036 | 3.001 | 1.005 | 1.996 | 3.001 |
| 2.2 | 0.391 | 0.935 | 2.067 | 3.002 | 1.013 | 1.989 | 3.002 |
| 2.3 | 0.5375 | 0.907 | 2.098 | 3.005 | 1.021 | 1.984 | 3.005 |
| 2.4 | 0.6617 | 0.881 | 2.127 | 3.008 | 1.030 | 1.978 | 3.008 |
| 2.5 | 0.76828 | 0.858 | 2.155 | 3.013 | 1.038 | 1.975 | 3.013 |
| 2.6 | 0.86037 | 0.835 | 2.181 | 3.016 | 1.046 | 1.970 | 3.016 |
| 2.7 | 0.94034 | 0.810 | 2.211 | 3.021 | 1.055 | 1.967 | 3.022 |
| 2.8 | 1.010114 | 0.788 | 2.239 | 3.027 | 1.063 | 1.964 | 3.027 |
| 2.9 | 1.071375 | 0.763 | 2.271 | 3.034 | 1.073 | 1.961 | 3.034 |
| 3.0 | 1.125454 | 0.721 | 2.330 | 3.051 | 1.092 | 1.959 | 3.051 |

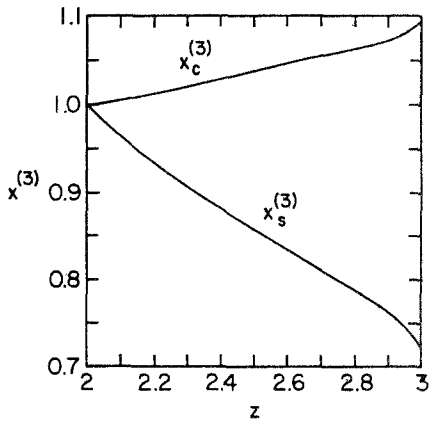


Fig. 11. The scaling exponents $x_s^{(3)}$ and $x_c^{(3)}$ as a function of $z$ for $2 \leqslant z \leqslant 3$.

small to exclude the possibility that it is in fact a constant. When $z > 3$, it was found that the exponents at the disappearance and reappearance points are equal and the same as those in the standard map. They are also independent of $z$ (see Table IV). Thus $z = 3$ plays a role similar to that of the upper critical dimension in phase transitions. It is, however, not clear what causes this change in behavior in the transition from $z < 3$ to $z > 3$.

For all cases of $z$ there are two common points to be noted. The first point is that the scaling exponents on the various nondominant symmetry lines are the same approximately, yet they are different from those on the dominant symmetry line. The sum of the two scaling exponents seems to be a constant (see Table V). The second point is that the convergence of

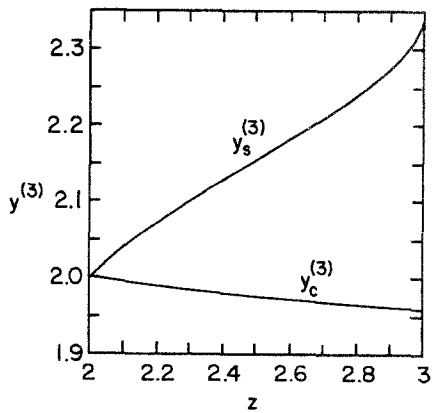


Fig. 12. The scaling exponents $y_s^{(3)}$ and $y_c^{(3)}$ as a function of $z$ for $2 \leqslant z \leqslant 3$.

**Table IV. Disappearance ($k_D$) and Reappearance ($k_R$) Points and the Scaling Exponents for $z > 3$**

| $z$ | $k$ | $x_s^{(3)}$ | $y_s^{(3)}$ | $x_s^{(3)} + y_s^{(3)}$ | $x_a^{(3)}$ | $y_a^{(3)}$ | $x_a^{(3)} + y_a^{(3)}$ |
|---|---|---|---|---|---|---|---|
| 3.8 | $k_D^{(1)} = 1.38253450$ | 0.7284 | 2.3261 | 3.0545 | 1.0990 | 1.9448 | 3.0438 |
| | $k_R^{(1)} = 1.38760367$ | 0.7226 | 2.3295 | 3.0521 | 1.1018 | 1.9512 | 3.0530 |
| 4 | $k_D^{(1)} = 1.41293530$ | 0.7219 | 2.3287 | 3.0506 | 1.1045 | 1.9419 | 3.0464 |
| | $k_R^{(1)} = 1.42173415$ | 0.7223 | 2.3281 | 3.0504 | 1.1015 | 1.9466 | 3.0481 |
| | $k_D^{(2)} = 1.42615570$ | 0.7203 | 2.3329 | 3.0533 | 1.0986 | 1.9425 | 3.0412 |
| 5 | $k_D^{(1)} = 0.80993000$ | 0.7234 | 2.3281 | 3.0515 | 1.1030 | 1.9432 | 3.0462 |
| | $k_R^{(1)} = 1.05287350$ | 0.7216 | 2.3288 | 3.0504 | 1.1040 | 1.9432 | 3.0472 |
| | $k_D^{(2)} = 1.39647420$ | 0.7221 | 2.3285 | 3.0505 | 1.1044 | 1.9422 | 3.0466 |
| 6 | $k_D^{(1)} = 0.70400046$ | 0.7218 | 2.3289 | 3.0507 | 1.1046 | 1.9421 | 3.0467 |
| | $k_R^{(1)} = 1.29946540$ | 0.7227 | 2.3284 | 3.0511 | 1.1037 | 1.9432 | 3.0470 |
| | $k_D^{(2)} = 1.43731867$ | 0.7228 | 2.3304 | 3.0532 | 1.1121 | 1.9327 | 3.0448 |
| | $k_R^{(2)} = 1.45296340$ | 0.7229 | 2.3303 | 3.0533 | 1.1121 | 1.9326 | 3.0447 |
| | $k_D^{(3)} = 1.51257548$ | 0.7221 | 2.3293 | 3.0513 | 1.1024 | 1.9454 | 3.0478 |
| 11 | $k_D^{(1)} = 0.27830553$ | 0.7211 | 2.3303 | 3.0515 | 1.1021 | 1.9462 | 3.0483 |

period-3 scaling is better than that of period-1 scaling (see Table VI). As a matter of fact, since the even and odd combinations of $(Q_i, P_i)$ in the Fibonacci sequence have period 3, period-3 scaling seems more natural. Further evidence is that at the critical values of $k$ the residues intersect at different values of $R^{\pm}$ according to the even and odd combinations of $(Q_i, P_i)$. On the nondominant symmetry line it was believed[2] that the scaling behavior is period-3. But on the dominant symmetry line it cannot be affirmed whether the scaling behavior is period-1 or period-3 from our

**Table V. Scaling Exponents on the Nondominant Symmetry Line at $k_D^{(1)} = 1.4129353$ for $z = 4$**

| $Q_i$ | $x_a^{(3)}$ | $y_a^{(3)}$ | $x_a^{(3)} + y_a^{(3)}$ | $x_b^{(3)}$ | $y_b^{(3)}$ | $x_b^{(3)} + y_b^{(3)}$ | $x_c^{(3)}$ | $y_c^{(3)}$ | $x_c^{(3)} + y_c^{(3)}$ |
|---|---|---|---|---|---|---|---|---|---|
| 4181 | 1.1105 | 1.9390 | 3.0495 | 1.0892 | 1.9620 | 3.0512 | 1.0888 | 1.9630 | 3.0518 |
| 6765 | 1.1090 | 1.9367 | 3.0457 | 1.0886 | 1.9642 | 3.0528 | 1.0887 | 1.9634 | 3.0521 |
| 10946 | 1.1067 | 1.9400 | 3.0467 | 1.0902 | 1.9603 | 3.0505 | 1.0881 | 1.9636 | 3.0517 |
| 17711 | 1.1050 | 1.9415 | 3.0465 | 1.0913 | 1.9623 | 3.0536 | 1.0904 | 1.9592 | 3.0496 |
| 28657 | 1.1037 | 1.9414 | 3.0451 | 1.0902 | 1.9633 | 3.0535 | 1.0900 | 1.9637 | 3.0537 |
| 46368 | 1.1027 | 1.9448 | 3.0475 | 1.0912 | 1.9581 | 3.0493 | 1.0905 | 1.9622 | 3.0526 |

**Table VI. Period-1 and Period-3 Scaling Exponents on the Dominant Symmetry Line $d$ at $k_D^{(1)} = 1.4129353$ for $z = 4$**

| $Q_i$ | $x_d^{(1)}$ | $x_d^{(3)}$ | $y_d^{(1)}$ | $y_d^{(3)}$ | $x_d^{(1)} + y_d^{(1)}$ | $x_d^{(3)} + y_d^{(3)}$ |
|---|---|---|---|---|---|---|
| 377 | 0.6998 | 0.7349 | 2.3325 | 2.3378 | 3.0323 | 3.0727 |
| 610 | 0.7373 | 0.7363 | 2.3812 | 2.3550 | 3.1185 | 3.0912 |
| 987 | 0.7332 | 0.7234 | 2.2788 | 2.3417 | 3.0120 | 3.0652 |
| 1597 | 0.7125 | 0.7277 | 2.3322 | 2.3249 | 3.0447 | 3.0526 |
| 2584 | 0.7243 | 0.7233 | 2.3609 | 2.3300 | 3.0852 | 3.0533 |
| 4181 | 0.7317 | 0.7228 | 2.2969 | 2.3334 | 3.0286 | 3.0562 |
| 6765 | 0.7127 | 0.7229 | 2.3301 | 2.3221 | 3.0428 | 3.0450 |
| 10946 | 0.7241 | 0.7228 | 2.3512 | 2.3298 | 3.0752 | 3.0526 |
| 17711 | 0.7270 | 0.7213 | 2.3072 | 2.3307 | 3.0342 | 3.0520 |
| 28657 | 0.7152 | 0.7221 | 2.3305 | 2.3251 | 3.0457 | 3.0472 |
| 46368 | 0.7218 | 0.7213 | 2.3451 | 2.3292 | 3.0669 | 3.0505 |

numerical data. It seems that both of them tend to the same limit, and different values of $R^{\pm}$ may eventually tend to the same limit as $Q_i \to \infty$. In Fig. 2, the residue curves for $z = 2$ first bunch into two groups according to the type of $(Q_i, P_i)$, and both of them then tend to zero as $k \to 0$. However, no matter what the scaling behavior is, period-3 scaling still has the advantage of giving faster convergence.

## 5. SUMMARY

The study of KAM tori in nonanalytic twist maps has revealed a surprisingly rich set of novel features. The behavior of KAM tori can change abruptly as one smoothly changes the degree of inflection $z$. Our results suggest that for $k > 0$, $z = 3$ is a major transition point in functional space, similar to that of the upper critical dimension in phase transitions. At this point the behavior of the "golden-mean" KAM torus is basically the same as that in the standard map. This is not surprising, since the algebraic function used here is merely the lowest order polynomial approximation to the sine function. For $z < 3$, there is no recurrence of KAM tori, and the scaling exponents vary with $z$. As $z$ is decreased from 3 to 2, the critical point decreases to zero, and the scaling exponents change smoothly from those of the standard map to those of a linear system. For $z > 3$ the KAM torus experiences a sequence of disappearance and reappearance as $k$ is increased. This recurrence may happen many, even infinitely many, times. The scaling exponents at the disappearance and reappearance points are the same as those in the standard map, and they are independent of $z$.

The many novel features observed in this work suggest that the behavior of KAM tori may in fact be much more complicated than we have been accustomed to think. It is thus worthwhile to conduct a more thorough study of the KAM theorem as well as the Greene criterion. Hopefully, the necessary conditions for their validity can also be found. The value of such a study lies not only in its intrinsic importance, but also its potential applications.

## ACKNOWLEDGMENTS

This work was supported in part by the U.S. Department of Energy under grant DE-FD05-87ER40374 and the Houston Area Research Consortium supercomputer grant 88-017.

## REFERENCES

1. J. M. Greene, *J. Math. Phys.* **20**:1183 (1979).
2. L. P. Kadanoff, *Phys. Rev. Lett.* **47**:1641 (1981); S. J. Shenker and L. P. Kadanoff, *J. Stat. Phys.* **27**:631 (1982).
3. R. S. MacKay, *Physica D* 7:283 (1983).
4. B. Hu and J. M. Mao, *Phys. Rev. A* **25**:3259 (1982); B. Hu and I. Satija, *Phys. Lett. A* **98**:143 (1983).
5. S. Ostlund, D. Rand, J. Sethna, and E. Siggia, *Physica D* **8**:303 (1983).
6. B. Hu, A. Valinia, and O. Piro, *Phys. Lett. A* **144**:7 (1990).
7. H. J. Schellnhuber and H. Urbschat, *Phys. Rev. Lett.* **54**:588 (1985).
8. J. Wilbrink, *Physica D* **26**:385 (1987).
9. J. A. Ketoja and R. S. MacKay, *Physica D* **35**:318 (1989).
10. J. N. Mather, *Math. Publ. IHES* **63**:163 (1982); *Erg. Th. Dyn. Sys.* **4**:301 (1984).